Angular correlation in the two-electron continuum

A. S. Kheifets
*Research School of Physical Sciences, The Australian National University, Canberra ACT 0200, Australia**

I. Bray
Centre for Atomic, Molecular, and Surface Physics, Physics and Energy Studies, Murdoch University, Perth, 6150 Australia †

(Dated: August 12, 2005)

Following absorption of a single photon, angles of simultaneous emission of two electrons from a He(n^1S) atom become more correlated with increasing n. We find that the strength of this correlation is due to the two-electron continuum of the electron-impact ionization of the $He^+(ns)$ ion. The strength is determined by the width of the momentum profile of the ionic ns state, and thus, somewhat counter-intuitively, depends inversely with the strength of the electron correlation in the He initial state. This explains the increasing (over He) angular correlation strength found in double photoionization of targets such as Be, Ne and H_2.

Correlated many-body dynamics in quantum systems is a topic of particular interest with implications spanning physics, chemistry and biology alike. A short list of most intriguing issues include mechanisms of high-T_c superconductivity [1], wave packet dynamics and femtochemistry [2], and electron-impact induced DNA strand break [3]. Fundamental processes like double photoionization (DPI), especially in the He atom, play a central, benchmarking role in this context. Understanding the role of electron correlations in this seemingly simple process, involving two electrons, provides insights to electron correlations in more complex breakup processes in many-electron systems.

Since the pioneering work of Wannier dated back more than 50 years ago [4], it has been established that the two-electron break-up is a tightly correlated process with the back-to-back emission being the only possible route to double ionization at the threshold. At a small excess energy E above the threshold, the electron pair acquires some dynamical freedom and can deviate from the back-to-back emission $\theta_{12} = \pi$ within a Gaussian distribution $\exp\left[-2\ln 2(\pi - \theta_{12})^2/\Delta\theta_{12}^2\right]$ with a finite angular correlation width $\Delta\theta_{12} \propto E^{1/4}$ [5, 6]. This result is based on the solution of the two-electron Schrödinger equation in the so-called Coulomb zone where the potential energy dominates over the kinetic energy and the two-electron escape follows closely the Wannier ridge $r_1 \simeq r_2$ and $\theta_{12} \simeq \pi$. At a sufficiently large separation $R = (r_1^2 + r_2^2)^{1/2}$, in the "far zone", the kinetic energy becomes dominant and the Coulomb force is not able to return the electrons back to the nucleus. The angular correlation width in the far zone remains unchanged until the electrons reach the detectors and it is this correlation width that determines the experimentally measured fully-differential cross-section. At small separations R, the Coulomb zone borders with the "interaction zone". In this zone, details of the interaction of the two-electron system with the external field become important. These details, however, are completely ignored in the Wannier theory since they do not affect the threshold law.

In the Wannier picture, we can view the Coulomb zone as a "two-electron collimator". The two electrons enter it from the side of the interaction zone with a wide spread of mutual angles θ_{12} but leave it into the far zone with the mutual angles tightly focused around $\theta_{12} = \pi$. As the energy of the electron pair decreases, the outer boundary of the Coulomb zone stretches to larger distances and its "collimating efficiency" increases resulting in decreasing angular correlation width $\Delta\theta_{12} \propto E^{1/4}$. The Wannier theory makes this prediction completely ignoring many-electron processes in the interaction region. Although these processes do not change the functional $E^{1/4}$ dependence, they can strongly modify the pre-exponential constant of proportionality.

In this Letter we analyze the processes in the interaction region from the point of view of their effect on the strength (size of $\Delta\theta_{12}$) of the angular correlation in DPI. Without too much loss of generality, we consider the He atom in a range of initial n^1S states for $n \leq 3$. For $n = 1$ we have the extreme of a highly correlated initial state. For $n = 3$ we have a rather diffuse initial state. We expect that any systematic, as a function of n, behavior here will translate well to more complex targets. In particular, we are motivated by trying to understand the narrowing of the DPI angular correlation width in Be [7, 8], Ne [9] and H_2 [10, 11].

Near the threshold, the DPI proceeds primarily via one electron absorbing the photon and then ionizing the residual ion via collisional impact. The DPI process is most probable if the photon is absorbed by an "inner" electron which then ejects an "outer" one. In this configuration, the recoil momentum is most readily accommodated by the nucleus [12]. At a small excess energy, the "outer" electron has sufficient time to adjust itself to a slow departure of the inner electron and thus remains in the ns ionic Thus, in the case of the He(n^1S) target the DPI process, after photon absorption, proceeds via

*Electronic address: A.Kheifets@anu.edu.au
†Electronic address: I.Bray@murdoch.edu.au

electron-impact ionization of the corresponding $He^+(ns)$ ion. We may also calculate $\Delta\theta_{12}$ explicitly for the e-$He^+(ns)$ system. If there is a strong similarity with the $\Delta\theta_{12}$ of the DPI then we can exclude the electron-electron correlations in the He initial n^1S state from contributing to the $\Delta\theta_{12}$ of the DPI.

We perform numerical calculations of the angular correlation width in the two-electron continuum using the convergent close-coupling (CCC) method. The DPI calculations have been described earlier [13, 14]. The only difference introduced here is the use of the box-space basis states [15] which allowed us to approach the double ionization threshold to within 0.4 eV.

The derivation of the angular correlation width for the electron-impact ionization is similar to DPI. We write the amplitude of the electron impact ionization of the target state i in the form of a partial wave expansion [16]:

$$f_i^S(\boldsymbol{k}_1,\boldsymbol{k}_2) = \frac{1}{\sqrt{4\pi}}\frac{1}{\hat{l}_i}\sqrt{\frac{k_0}{k_1}}\sum_{l_0 l_1 l_2 J}(2l_0+1)^{1/2} \times C^{Jm_i}_{l_0 0\ l_i m_i}\, T^{JS}_{l_0 l_1 l_2}(k_1,k_2)\, \mathcal{Y}^{l_1 l_2}_{Jm_i}(\boldsymbol{k}_1,\boldsymbol{k}_2) \quad (1)$$

Here, the projectile of momentum $\boldsymbol{k}_0$ is directed along the quantization z-axis and the total spin of the scattering system is S. The T-matrix entering Eq. (1) is obtained by the projection of the true continuum state $\boldsymbol{k}_2$ onto the same-energy pseudostate:

$$T^{JS}_{l_0 l_1 l_2}(k_1,k_2) = (-i)^{l_0+l_1+l_2} e^{i(\delta_{l_0}+\delta_{l_1}+\delta_{l_2})} \times \langle k_2 l_2 \| n l_2\rangle\, \langle k_1\phi_n \| T^{JS} \| \phi_i k_0\rangle \quad (2)$$

Here $\langle k_1\phi_n\|T^{JS}\|\phi_i k_0\rangle$ is the bare T-matrix stripped of all phase factors and angular momentum projections.

We shall restrict ourselves to the dipole singlet amplitude which is the only amplitude relevant to DPI. In this case for an s target state $l_i = 0$, $l_0 = 1$, $J = 1$ and Eq. (1) can be further simplified:

$$f_{sp}(\boldsymbol{k}_1,\boldsymbol{k}_2) = \sqrt{\frac{3}{4\pi}}\sqrt{\frac{k_0}{k_1}}\sum_{l_1 l_2} T_{l_1 l_2}(k_1,k_2)\, \mathcal{Y}^{l_1 l_2}_{10}(\boldsymbol{k}_1,\boldsymbol{k}_2)\ , \quad (3)$$

where $l_2 = l_1 \pm 1$. The (e,2e) cross-section is given by the squared amplitude (3):

$$\frac{d\sigma_{sp}}{d\Omega_1 d\Omega_2 dE_2} = (2\pi)^4 \frac{k_1 k_2}{k_0}|f_{sp}(\boldsymbol{k}_1,\boldsymbol{k}_2)|^2, \quad (4)$$

After we introduce symmetric and antisymmetric combinations of the T-matrices:

$$T^{\pm}_{l_1 l_2}(E_1,E_2) = \frac{1}{2}\left\{T_{l_1 l_2}(E_1,E_2) \pm T_{l_1 l_2}(E_2,E_1)\right\}, \quad (5)$$

the angular momentum summation in (3) can be reduced to the sum over a single variable. This allows us to parametrize the cross-section (3) in the form:

$$\frac{d\sigma_{sp}}{d\Omega_1 d\Omega_2 dE_2} \propto \Big|(k_{1z}+k_{2z})g^+(E_1,E_2) + (k_{1z}-k_{2z})g^-(E_1,E_2)\Big|^2, \quad (6)$$

where the symmetric and antisymmetric amplitudes are

$$g^{\pm}(E_1,E_2) = \frac{1}{4\pi}\sum_{l=0}^{\infty}\frac{(-1)^l}{\sqrt{l+1}}\left[P'_{l+1}(\cos\theta_{12}) \mp P'_l(\cos\theta_{12})\right] \times T^{\pm}_{ll+1}(E_1,E_2). \quad (7)$$

Here we used expressions for the bipolar harmonics $\mathcal{Y}^{l_1 l_2}_{10}$ due to Manakov et al. [17]. The mutual electron angle is defined by $\cos\theta_{12} = \hat{k}_1 \cdot \hat{k}_2$. We note that Eq. (7) is identical to Eq. (13) of Ref. [14] except for the T-matrix elements which are substituted by the dipole matrix elements in the DPI case.

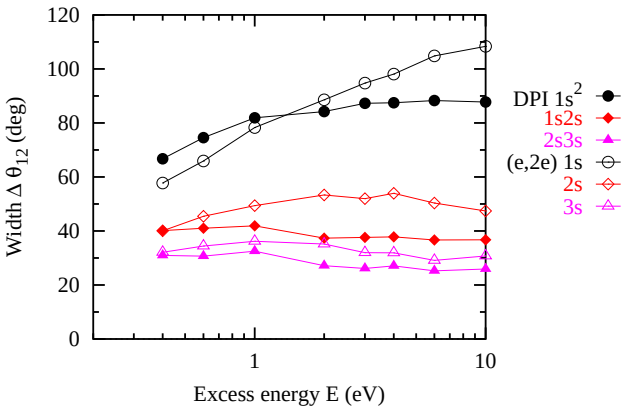

FIG. 1: Gaussian width parameters for DPI of $He(n^1S)$ and (e,2e) of $He^+(ns)$ for $n \le 3$ plotted versus excess energy over the corresponding double ionization threshold. Circles, diamonds, and triangles correspond to widths for the n=1, 2, and 3 initial states, respectively. Filled symbols are for DPI on He and open symbols are for (e,2e) on He^+.

We concentrate on the special case of equal energy sharing when g^- vanishes. Close to double ionization threshold, the symmetric amplitude can be fitted with the Gaussian ansatz:

$$|g^+| = A\ \exp\left[-2\ln 2\frac{(\pi-\theta_{12})^2}{\Delta\theta_{12}^2}\right] \quad (8)$$

where the Gaussian width parameter $\Delta\theta_{12}$ is the measure of strength of the angular correlation.

In Figure 1, we plot the Gaussian width parameters for DPI of the He atom in the n^1S initial states, where $n \le 3$, as functions of the excess energy over the corresponding double ionization threshold. In the same figure, we overplot the Gaussian width parameters for the electron impact ionization of the He^+ ion in the corresponding ns state.

We observe that there is a systematic reduction in the widths as n increases. The angular correlation widths of the two processes follow each other closely and for $n = 2$ and 3 merge near the threshold. This indicates that the angular correlation width in DPI is indeed dominated by the corresponding (e,2e) process. We fit the energy

dependent angular correlation width of the latter process by the Wannier threshold law

$$\Delta\theta_{12}(E) = C_n \times E^{1/4} \qquad (9)$$

where C_n is the angular correlation width at 1 eV excess energy and E is measured in eV. The energy-independent pre-exponential factors C_n are found to be 78°, 49°, and 38° for the n =1, 2, and 3 states of He^+, respectively.

We now demonstrate that the factor C_n is strongly related to the width of the momentum profile (squared momentum-space wave function $|R_{ns}(q)|^2$) of the target ion state being ionized. Indeed, it is well established in the (e,2e) reaction that the width of the angular distribution of the ejected electron is determined by the momentum profile of the target orbital [18, 19]. We plot these profiles in Figure 2. For better visibility, we normalize all the profiles to that of the ground state $1s$ orbital of He^+ ion. We see that the range of the possible momenta available in the bound state is rapidly decreasing from $1s$ to $3s$. Therefore, the total momentum of the two electrons after an ionizing collision, which determines the range of mutual angles in the interaction zone, will have the largest spread following ionization of the $1s$ ground state. We illustrate this dependence in Figure 3, where we plot the energy-independent pre-exponential factor C_n in Eq. (9) versus the width of the momentum profile at half maximum Δq of the corresponding H^+ ion state ns extracted from Figure 2. We see a very strong correlation which can be approximated by a power law $\Delta c_{12} \propto \Delta q^{0.4}$.

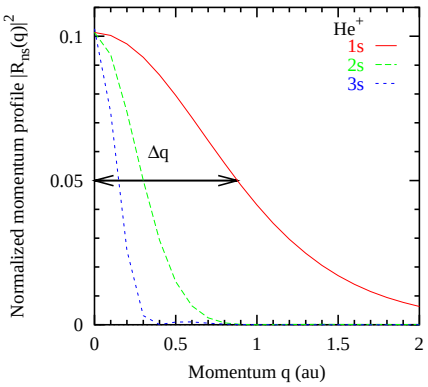

FIG. 2: Momentum profiles (squared momentum space wave functions) $|R_{ns}(q)|^2$ of the lowest ns states of the He^+ ion. The momentum profiles are normalized to $|R_{1s}|^2$ at its maximum.

From these findings we conclude that the strength of the angular correlation in DPI of $He(n^1S)$ comes primarily from the momentum distribution of the corresponding $He^+(ns)$ state. More specifically, the angular correlation width in DPI is a result of interplay of two distinct processes. It is initially set up in the interaction region during an ionizing collision of the photoelectron with the positively charged ion. This ionizing collision creates an

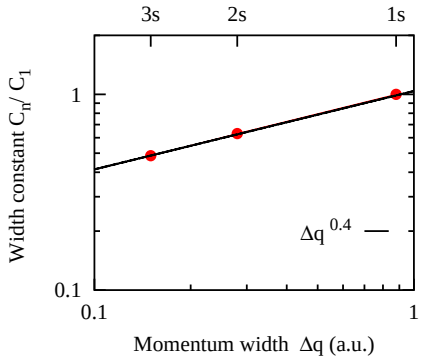

FIG. 3: Energy-independent width constants C_n in Eq. (9) plotted versus the width of the corresponding momentum profile extracted from Figure 2.

electron pair with the spread of mutual angles determined by the momentum profile of the target electron bound in the ion. Then the electron pair travels through the Coulomb zone which greatly reduces the spread of the mutual angles focusing them around 180°. As a result, the electron pair emerges in the far zone with the angular correlation width which depends on the size of the Coulomb zone (energy dependence $E^{1/4}$ in Eq. (9)) and the momentum profile of the bound ion state (energy-independent pre-exponential factor C_n).

According to this scenario, at the same excess energy above the double ionization threshold, the He atom in the ground state will have the largest angular correlation width of DPI due to the largest width of the momentum profile of the $1s$ state of the bare $Z = 2$ Coulomb centre. Hence we have the curious result that the strength of the angular correlation in the continuum varies inversely with this strength in the electron-electron correlation in the initial bound state. All other neutral atomic and molecular targets, after single ionization, will have lesser bound states either due to screening by other target electrons in atoms or a delocalized Coulomb centre in molecules. Therefore, these atomic and molecular targets will have smaller correlation widths of the DPI than say for He initially in the ground state.

The authors wish to thank Australian Partnership for Advanced Computing (APAC) and ISA Technologies, Perth, Western Australia, for provision of their computing facilities. Support of the Australian Research Council in the form of Discovery grant DP0451211 is acknowledged.

[1] J. Orenstein and A. J. Millis, Science **288**, 468 (2000).
[2] C. Daniel, J. Full, L. Gonzalez, C. Lupulescu, J. Manz, A. Merli, S. Vajda, and L. Woste, Science **299**, 536 (2003).
[3] B. Boudaiffa, P. Cloutier, D. Hunting, M. A. Huels, and L. Sanche, Science **287**, 1658 (2000).
[4] G. H. Wannier, Phys. Rev. **90**, 817 (1953).
[5] A. R. P. Rau, J. Phys. B **9**, L283 (1976).
[6] J. M. Feagin, J. Phys. B **17**, 2433 (1984).
[7] A. S. Kheifets and I. Bray, Phys. Rev. A **65**, 012710 (2002).
[8] F. Citrini, L. Malegat, P. Selles, and A. K. Kazansky, Phys. Rev. A **67**, 042709 (2003).
[9] P. Bolognesi, L. Avaldi, I. Bray, R. Camilloni, M. Coreno, K. Kazansky, A. Kheifets, L. Malegat, P. Selles, G. Turri, et al., Physica Scripta **T110**, 104 (2004).
[10] T. J. Reddish, J. P. Wightman, M. A. MacDonald, and S. Cvejanović, Phys. Rev. Lett. **79**, 2438 (1997).
[11] T. Weber, A. Czasch, O. Jagutzki, A. Müller, V. Mergel, A. Kheifets, J. Feagin, E. Rothenberg, G. Meigs, M. Prior, et al., Phys. Rev. Lett. **92**, 163001 (2004).
[12] M. Y. Amusia, E. G. Drukarev, V. G. Gorshkov, and M. O. Kazachkov, J. Phys. B **8**, 1248 (1975).
[13] A. S. Kheifets and I. Bray, Phys. Rev. A **62**, 5402 (2000).
[14] A. S. Kheifets and I. Bray, Phys. Rev. A **65**, 022708 (2002).
[15] I. Bray, K. Bartschat, and A. T. Stelbovics, Phys. Rev. A **67**, 060704(R) (2003).
[16] I. Bray and D. V. Fursa, Phys. Rev. A **54**, 2991 (1996).
[17] N. L. Manakov, S. I. Marmo, and A. V. Meremianin, J. Phys. B **29**, 2711 (1996).
[18] A. E. Glassgold and G. Ialongo, Phys. Rev. pp. 151–159 (1975).
[19] M. E. Rudd, Phys. Rev. A **44**, 1644 (1991).